

3-D seismic horizon map processing

Dan Vetrici and Robert R. Stewart

ABSTRACT

The 3-D seismic volume with the final 3-D seismic maps present a great opportunity for image processing. The limited readable information in these maps can be increased by subsequent digital image processing. Techniques of image processing have been employed in numerous geophysical fields, especially in gravity and magnetics. A review of digital image processing techniques also evaluates their applicability to 3-D seismic map enhancement. Digital image spatial and frequency enhancement are introduced and evaluated on Sierra BC 3-D seismic data.

INTRODUCTION

Image processing techniques are employed to achieve a specific interpretive goal - to uncover anomalies within an observed data set. A typical seismic interpretation workstation displays the seismic data and interpretation maps as images. In the process of seismic interpretation the geophysicist uses the seismic workstation, to correlate geological events with seismic discontinuities and produce two-way time and attribute maps to define anomalous areas with oil and gas potential. Image processing within the workstation is available to the interpreter as color palette, horizon smoothing, edge and dip detection.

Digital image processing techniques are applied in various fields from remote sensing imagery to the film and photo hobbies, from the simple spatial image enhancement to the sophisticated computer visualization and interpretation. A review of the digital image processing fundamentals in image enhancement is followed by a proposal of a method to extract further lithological information from the 3-D seismic data.

General

A full cycle of the seismic reflection method applied in oil exploration consists of acquisition, processing and interpretation phases. Currently these phases are continuously redesigned to the extent that the final product, the seismic interpreted (two way time horizon, isochron, seismic attribute, depth derived) map has the required accuracy to uncover the subsurface anatomy, to detect the "reservoir anomaly". The reservoir is usually indirectly characterized by comparison to historical cases. Seismic calibration, a frequent approach among seismic interpreters is based on well data and previous experience (either their own or from the literature).

Because of limitations of the seismic experiment, a processed data set does not explicitly contain the full geological information from the subsurface. The bandwidth of the P seismic signal and processing approximations are obstacles challenging seismic exploration.

New seismic acquisition and processing techniques are developed as seismologists strive to objectively extract geological information from the seismic data. AVO, seismic attribute analysis, and most recent 3-D coherency are seismic techniques expanding our geological description of the subsurface. As geophysicists obtain high quality seismic

data throughout acquisition and processing, seismic interpreters produce highly specialized maps and new methods will be available to perform enhanced geologic interpretation.

A 3-D seismic map, defined as a 2-D surface $g(x, y)$ can be treated as a digital image of a stratified but possibly laterally discontinuous rock body. The associated attribute (reflection strength, instantaneous phase, instantaneous frequency, weighted average frequency) contains information pertinent to the physical property contrast of this body and the overlaying sediments. In the space contained between two defined seismic surfaces (horizons) lateral lithological discontinuities occur. As seismic methods become more involved in the search for these variations, they might point to potential hydrocarbon reservoirs.

Digital image processing offers new tools in 3-D seismic interpretation. Digital image processing is currently used in 3-D seismic interpretation on workstation as color display, horizon smoothing, image operation (subtraction or addition), edge and azimuth detection and illumination. A review of digital processing techniques suggests potential applications in 3-D seismic interpretation.

In this paper, the image enhancement techniques tested are described.

IMAGE ENHANCEMENT TECHNIQUES.

Enhancement techniques are applied in the spatial domain, frequency domain or a combination of the two. The aim of these processes is to obtain a more suitable image than the original by manipulations of the pixel gray level distribution.

A digital image $f(x, y)$ can be defined as

$$f(x, y) = i(x, y) g(x, y),$$

where $i(x, y)$ is illumination, $0 < i(x, y) < 1$

$g(x, y)$ is reflectance, $0 < g(x, y) < 1$

The gray level (l) of an image $f(x, y)$ at a point of coordinates (x, y) is defined as its monochrome intensity at that point, $L_{\min} < l < L_{\max}$

The gray scale $[L_{\min}, L_{\max}]$ is the gray level interval of definition. In practice this interval is shifted to $[0, L]$ where $l = 0$ is considered black and $l = L$ is considered white in the scale.

Spatial domain methods.

Spatial domain refers to the aggregate of pixels in an image. Image processing in spatial domain can be expressed as

$$g(x, y) = T[f(x, y)]$$

where f is the input image, g is the processed image and T is the operator.

Point processing.

Intensity transformation:

- Image negatives: this process reverses the direction of intensity variation between the output and input images. The linear transformation is represented by

$$s = T(r) = a r + b$$

with r the gray level variable in the image to be enhanced and a and b constant.

- Contrast stretching

An increase in the dynamic range of the image output is achieved by modifying the threshold function of the original image without modifying the gray level order.

- Compression of dynamic range: an operator defined by

$$s = c(\log(1 + |r|)) \quad c = \text{scaling constant}$$

compresses effectively the dynamic range of pixel gray value.

- Gray level slicing refers to operating on the gray levels in the image related to feature of interest.

- Bit-plane slicing is a process to modify the contribution to the output image made by specific bits in the bit planes.

Histogram processing:

The histogram of a digital image with gray levels in the range $[0, L-1]$ is a discrete function $p(r) = n_k/n$, where r_k is the k th gray level, n_k is the number of pixels in the image, n is the total number of pixels in the image and $k = 0, 1, 2, \dots, L - 1$

- Histogram equalization is performed with an operator defined by

$$s_k = T(r_k) = \sum n_j / n$$

- Histogram specification is a process of implementation of a specified gray level density function in order to match the density function of a desired image. Histogram processing:

- Histogram specification is a process of implementation of a specified gray level density function in order to match the density function of a desired image.

Image subtraction

$$g(x, y) = f(x, y) - h(x, y)$$

Image averaging

Random noise η from an image

$$g(x, y) = f(x, y) + h(x, y)$$

can be removed by averaging M noisy images

$$g(x, y) = 1/M \sum f(x, y)$$

Spatial filters

Spatial filters or masks are employed in image enhancement techniques to modify the average contrast and intensity. The basic concept is to replace the gray level in a pixel by the combination of the mask coefficients and gray levels of the neighbor pixels covered by the mask centered on. A 3X3 mask response is the sum of the product of z_i the gray level of the pixel and w_i the mask coefficient at the pixel location

$$R = \sum w_i z_i$$

Smoothing filters

- Lowpass filtering: the central pixel gray level is the average of the mask gray level.

$$L_{\text{mask}} = 1/n^2 [n^2 (\text{ones})]$$

- Median filtering: the central pixel gray level is replaced by the median of the gray levels in the mask.

Sharpening filters:

- Highpass filtering: a mask with a central positive coefficient and negative outside will highlight the fine detail in an image. The mask coefficient sum is zero.

$$L_{\text{mask}} = -1/n^2 [(n^2-1) (-\text{ones}), w_{\text{central}}]$$

- Highboost filtering: enhances the high frequencies in an image.

- Derivative filtering: uses the gradient vector to restore original background and enhance edges. Roberts [1 0; 0 -1], [0 1; -1 0], Prewitt [-1 -1 -1; 0 0; 0; 1 1 1], [-1 -1 -1; 0 0; 0; 1 1 1], and Sobel [-1 -2 -1; 0 0; 0; 1 2 1], [-1 0 1; -2 0; 2; -1 0 1] operators are frequently used to approximate the gray level gradient.

Frequency-domain methods.

The methods of the image processing in the frequency domain are based on the convolution theorem. A processed image g obtained from an original image f convolved with a linear operator h can be expressed in the spatial domain

$$g(x, y) = h(x, y) * f(x, y)$$

and in the frequency domain with the correspondent 2-D Fourier transforms G , H and F

$$G(u, v) = H(u, v)F(u, v)$$

where $H(u, v)$ is the transfer function of the process and is computed in a way that in the resultant image $g(x, y)$ features of interest are enhanced.

Smoothing filters:

Lowpass filtering

a) Ideal filter is a filter which passes all frequencies in a band width no attenuation.

$$H(u, v) = 1 \quad D(u, v) < D_0$$

$$D(u, v) = (u^2 + v^2)^{1/2}$$

b) Butterworth filter

$$H(u, v) = 1 / (1 + [D(u, v) / D_0]^{1/2})$$

Sharpening filters:

Highpass filtering:

a) Butterworth filter

$$H(u, v) = 1 / (1 + [D(u, v) / D_0]^{1/2})$$

b) Homomorphic filtering

$$g(x, y) = e [s(x,y)]$$

COLOR IMAGE PROCESSING

Color image processing is applied to exploit the human eye capability to differentiate colors comparative to the gray scale and to make use of the color as a descriptor in object identification and extraction.

Color attributes are brightness (intensity), hue (dominant wavelength of a color) and saturation (purity of white light mixed with hue). Any color is defined by the red (X), green (Y) and blue contributions (Z) as

$$x = X/(X + Y + Z) \quad y = Y/(X + Y + Z) \quad z = Z/(X + Y + Z)$$

$$x + y + z = 1$$

Pseudo-color processing

- Intensity slicing: colors are subjective assigned to pixels with gray levels in a defined interval.

- Gray level to color transformation: is based on three independent transformations on the gray level of the pixel input and assigned a red, green and blue output..

Full color processing

- HSI (hue, saturation, intensity) images from an RGB (red, green, blue) image is performed to enhance the color sensing properties of the human eye to perform specialized tasks.

- HSI modeling is based on the separation of the intensity component from the color information in an image. An image is processed in HSI format and reconverted in RGB for display.

IMAGE RESTORATION

This is a process that attempts to recover an image that has been degraded by using some a priori knowledge of the degradation phenomenon.

Degradation process is an operator or a system H , which together with an additive noise term $h(x, y)$ operates on input image $f(x, y)$ to produce a degraded image $g(x, y)$.

Techniques of image restoration applied to the seismic data are subject for further work. A list of these methods includes: 1) Unconstrained restoration, 2) Constrained restoration, 3) Inverse filtering, 4) Last square filter, 5) Restoration in spatial domain and 6) Geometric transformation.

Seismic data is always subjected to degradation and developing new tools to minimize the loss of information are beneficial to the geophysicist. At this time we test image enhancement data using spatial and frequency filters designed to respond to a particular data set.

EXPERIMENTAL DATA

We present a sequence of images from the Sierra 3-D seismic data and experiment with digital image processing. From the Landmark workstation, interpreted data such as seismic two-way time and amplitude horizons and time slices are exported into Matlab for processing. Macintosh Adobe Photoshop software packages was used for graphic presentation in this work.

The Sierra gas field covered by this 3-D seismic survey is one of the largest gas accumulations in Western Canada. Gas is produced from the Keg River carbonate buildup. The geology of this field is well known and we refer to Torrie (1973) for the geological information. The field is declining and more water is produced. Seismic data was acquired to evaluate the carbonate reservoir.

Sierra reef geology

Sierra reefs developed in an area of Northern Interior Plains which throughout its early geological history was in a position relative to the western geosyncline with the deeper neritic sediments located to the west. From late Jurassic to Paleocene the Rocky Mountains formed.

The economic basement arbitrarily set as the Cambro-Ordovician quartzities is overlaid by Devonian, Mississippian and Permian sediments.

During Middle Devonian, a major barrier-reef system had developed, separating back-reef Muskeg carbonates and evaporites from the fore-reef Outer Park shales and

carbonates. During the initial growth phase, the Upper Keg River, a complex system of barriers, mounds and pinnacle reef basins, developed in a position back-reef to the main barrier system. Lower Muskeg carbonates and evaporites were then deposited. Reef growth continued on the main barrier up to the base of Slave Point with Muskeg carbonate and evaporate deposition continuing south of the barrier.

General emergence, marked by the Watt Mountain shale and limestone breccias terminated Upper Elk Point reef growth. The final stage of Middle Devonian reef growth, the Slave Point, is commonly offset seaward from the Elk Point barrier reef. The Slave Point reef separates fore-reef Otter park shale from back-reef Slave Point limestone.

Sierra reef characteristics

Location	NE British Columbia, 58 ⁰ 50'N, 121 ⁰ 20'W
Age	Eifelian - Givetian, Pine Point Formation
Reef Type	platform reef
Dimensions	7000m (NW-SE) and 3000m (NE-SW)
Depth sub sea level	1500 m
Depositional Setting	shelf slope and basin
Tectonic Region	High River Shelf
Crustal Position	craton margin
Foundation below Reef	Keg River carbonate platform (? on basement highs)
Bathymetric Range	shallow subtidal to supratidal
Reef forming Process	lower, periodic growth of stromatoporoid reef; upper, stacking of shallowing upward cycles
Dominant Organism(s)	stromatoporoids, algae
Diagnostic Aspects	2-part lithology; lower dolomitized reef upper limestone reef and associate facies
Porosity	average 10%; vugs and fractures, mainly in dolomite
Character of Fluids	sour gas, salt water
Original Raw Gas in Place	1.10 Tcf
Raw Gas produced to date	0.80 Tcf
Drilled Wells	6 wells

Seismic data

Conventional reflection seismic processing usually assume: 1) horizontal layers of constant velocity, and 2) compressional plane wave that reflects on layer boundary at normal incidence, no shear waves are generated. Real 3-D data after processing contains information pertinent to the subsurface which is of course not always flat and has other elastic events.

The Sierra 3-D seismic grid (Figure 1) consists of 289 lines and 468 crosslines. The data are of average resolution and at this time we do not have access to the field records. At the first inspection amplitude distortion along the WE lines was observed on the interpreted horizons, larger at shallow depths. Compare Tetcho (700 ms Figure 2) with Slave Point (time 1100 ms, Figure 3).

The gray level discussed in the digital image processing section is now related to specific seismic measurements: two way time, seismic amplitude real or complex.

Seismic horizon map processing

The 3-D seismic horizons interpreted in Landmark are exported to Matlab for 2-D processing. Data transfer was executed in ascii format. Filters designed with the Seismic Signal Processing tools are applied to the input data.

One of the difficulties to apply the image processing techniques on the Sierra 3-D seismic data was the irregular seismic coverage. Two dimensional processing is performed optimally on square arrays. In this experiment the seismic data was prepared for processing regarded as a sparse matrix. Another approach might be that of decomposing data in square "images", processed separately and the final results pasted together.

The histogram function was calculated at any step in experiment. The Sierra data seismic images are rated as low contrast pictures.

Enhancement processing

Tetcho and Slave Point are the two-way time horizons input data. The carbonate buildup structure is first expressed at the Slave Point time. The horizon data are filtered with low-pass and high-pass filters and the results show little improvement over the original.

The input time slice TS 1150, Figure 4 was processed with low-, high- and gradient filters in the space and frequency domain. Special displays with different color processing bring up more detailed.

A 3X3 high-pass filter (Figure 5) does a remarkable job. The power spectrum of the new image is displayed in Figure 6.

The gradient operators Roberts (Figure 7), Prewitt (Figure 8) and Sobel (Figure 9) filters are applied for edge detection. The reef edge is well contoured in all these enhanced images.

The averaged sum of five time slices from 1110 to 1150 ms is displayed in Figure 10. The grid noise is not canceled but even is enhanced. Radar digital image processing techniques employs destriping tools.

Acoustic impedance map

The amplitude of the seismic trace $A = A(x, y, t)$ at the boundary between two acoustic media, for normal incidence is defined as

$$A_{i-1, i} = [\rho_i V_i - \rho_{i-1} V_{i-1}] / [\rho_i V_i + \rho_{i-1} V_{i-1}]$$

$$A_{i, i+1} = F\{[k - \rho_i V_i] / [k + \rho_i V_i]\}$$

$$A_{i+1, i+2} = k = F(\rho_{i+1}, V_{i+1})$$

$$F(\rho_i V_i) = k [1 - A_i(x, y)] / [1 + A_i(x, y)]$$

$$\text{with } \rho = \rho(x, y, t) \text{ and } V = V(x, y, t)$$

(x, y) can be estimated from well data and the velocity at the observed time is estimated by the acoustic impedance distribution. The normalized amplitudes for a time slice as a horizon "acoustic impedance" map is defined as

$$\rho_i(x, y) V_i(x, y) = k \sum [1 - A_i(x, y)] / [1 + A_i(x, y)]$$

For the Sierra field we used the sonic and density well logs to estimate the seismic amplitude and normalize the horizon impedance. The acoustic impedance if properly calibrated is a good reservoir measurement. Figure X displays two acoustic impedance time slices processed as described

Coherency map

The coherency between two signals x and y is a function of the power spectra of the signals and their cross spectrum

$$C_{xy}(l, m) = [P_{xy}(l, m)]^2 / [P_{xx}(l, m) P_{yy}(l, m)]$$

Figure 11 is a three-term coherency map on the 1150 time slice. A coherency function between time slices will be tested and probably implemented for a larger data volume.

CONCLUSIONS

The image processing techniques applied to the 3-D Sierra seismic data demonstrate the power of the 2-D filters to obtain higher quality displays within a 3-D seismic volume. A consecrated image processing package will facilitate faster and more flexible computations.

Qualitative interpretation is further performed using acoustic impedance maps derived from the normalized amplitude.

Once the flow of a image processing is designed the full 3-D seismic volume can be processed and reinterpretation on vertical and horizontal sections performed.

ACKNOWLEDGMENT

We acknowledge Mobil Oil Canada support for releasing the Sierra 3-D seismic survey to the Department of Geology and Geophysics at University of Calgary.

REFERENCES

- Billingsley, P., 1986, Probability and measure, John Wiley & Sons.
- Brown, A. R., 1991, Color, character and zero-phasesness: Interpretation of 3-dimensional seismic data, AAPG Memoir 42, 21-41.
- Clarkson, M. P., and Stark, H., 1995, Signal processing methods for audio, images and telecommunications, Academic Press.
- Gonzales, R. C., and Woods, R. E., 1993, Image restoration: Digital image processing, Addison-Wesley.
- Phipps, G., 1982, Exploring for dolomitized Slave Point carbonates in northeastern British Columbia: JCSEG 18, 7-13.
- Richards, J. A., 1993, Remote sensing digital image analysis, An introduction, Springer Verlag.
- Torrie, J. E., 1973, Northeastern British Columbia, Future Petroleum Provinces of Canada, Memoir 1, CSPG, 151-186.
- Yilmaz, O., 1988, 2-D surface processing: Seismic data processing, SEG, 491-495.

FIGURES

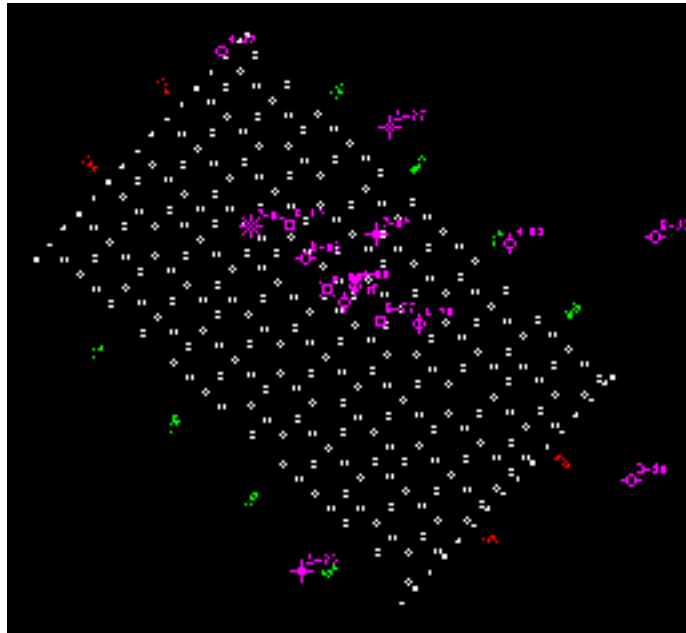


Figure 1. Sierra 3-D survey shot point map

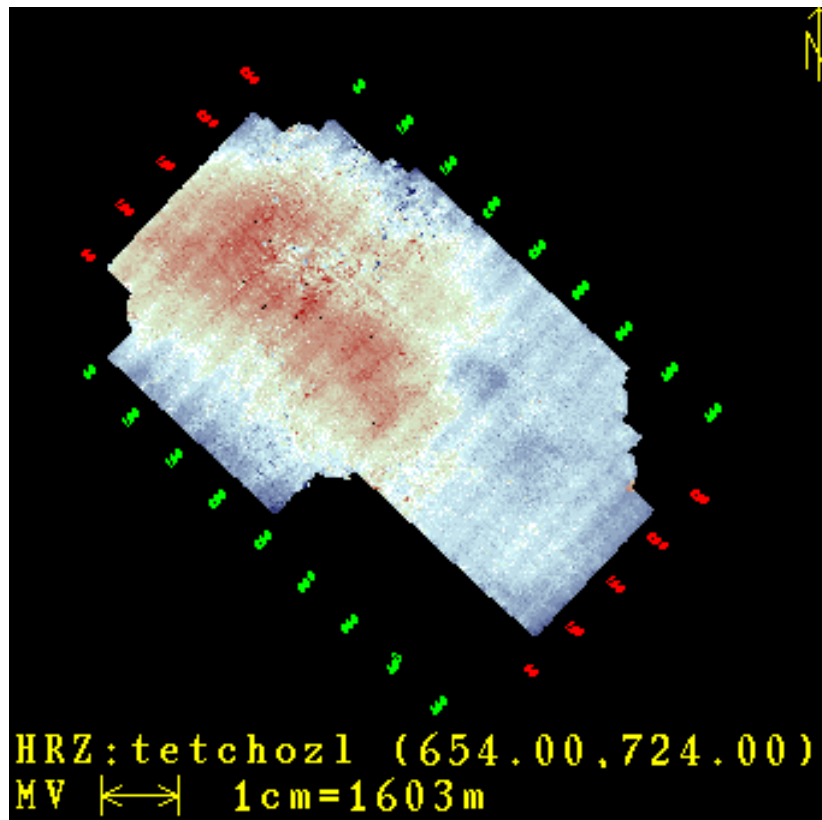


Figure 2. Sierra Tetcho two-way time horizon - input data.

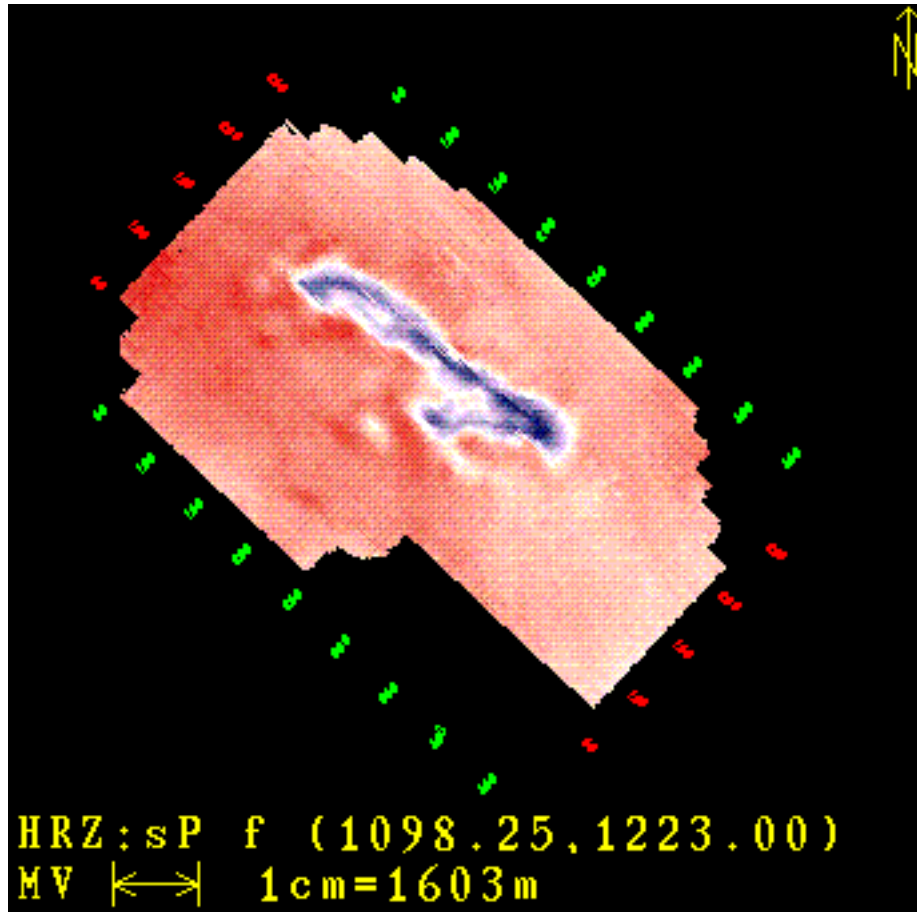


Figure 3. Sierra - Slave Point two-way time horizon - input data.

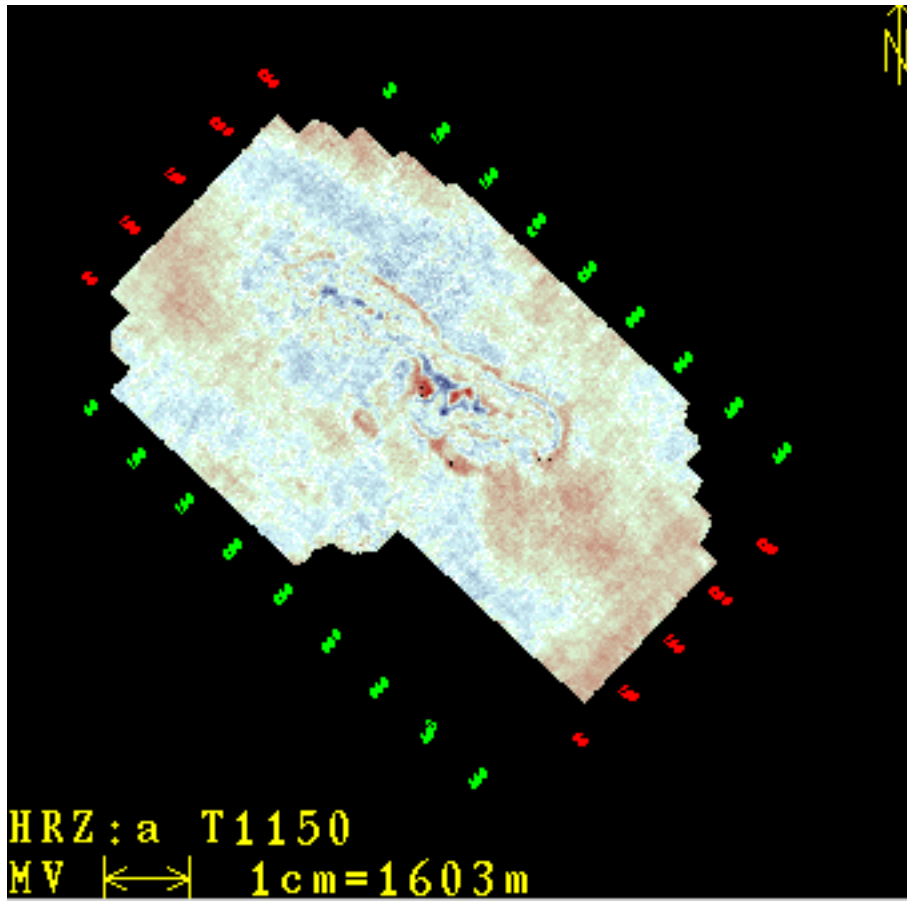


Figure 4. Sierra Time slice at 1150 ms- input image.

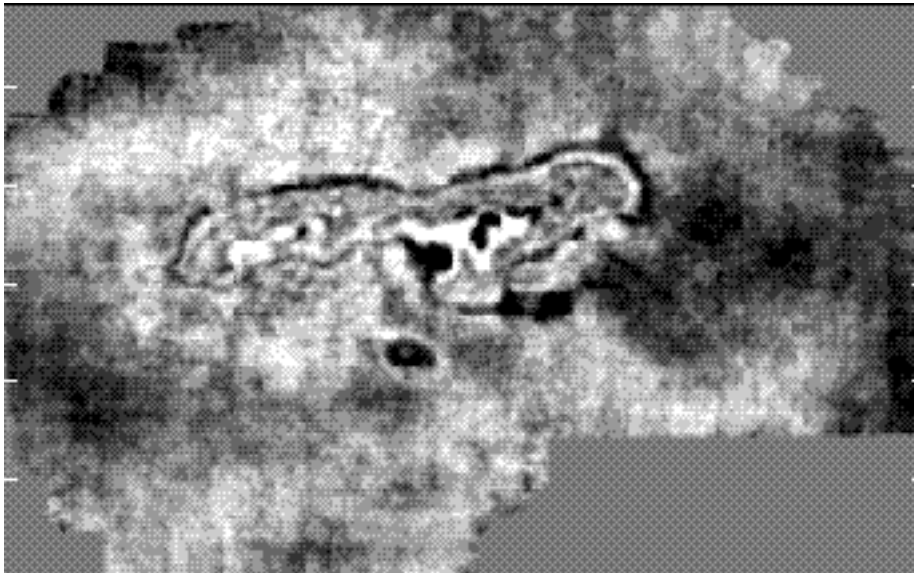


Figure 5. Sierra Time slice at 1150 ms filtered with highpass filter.

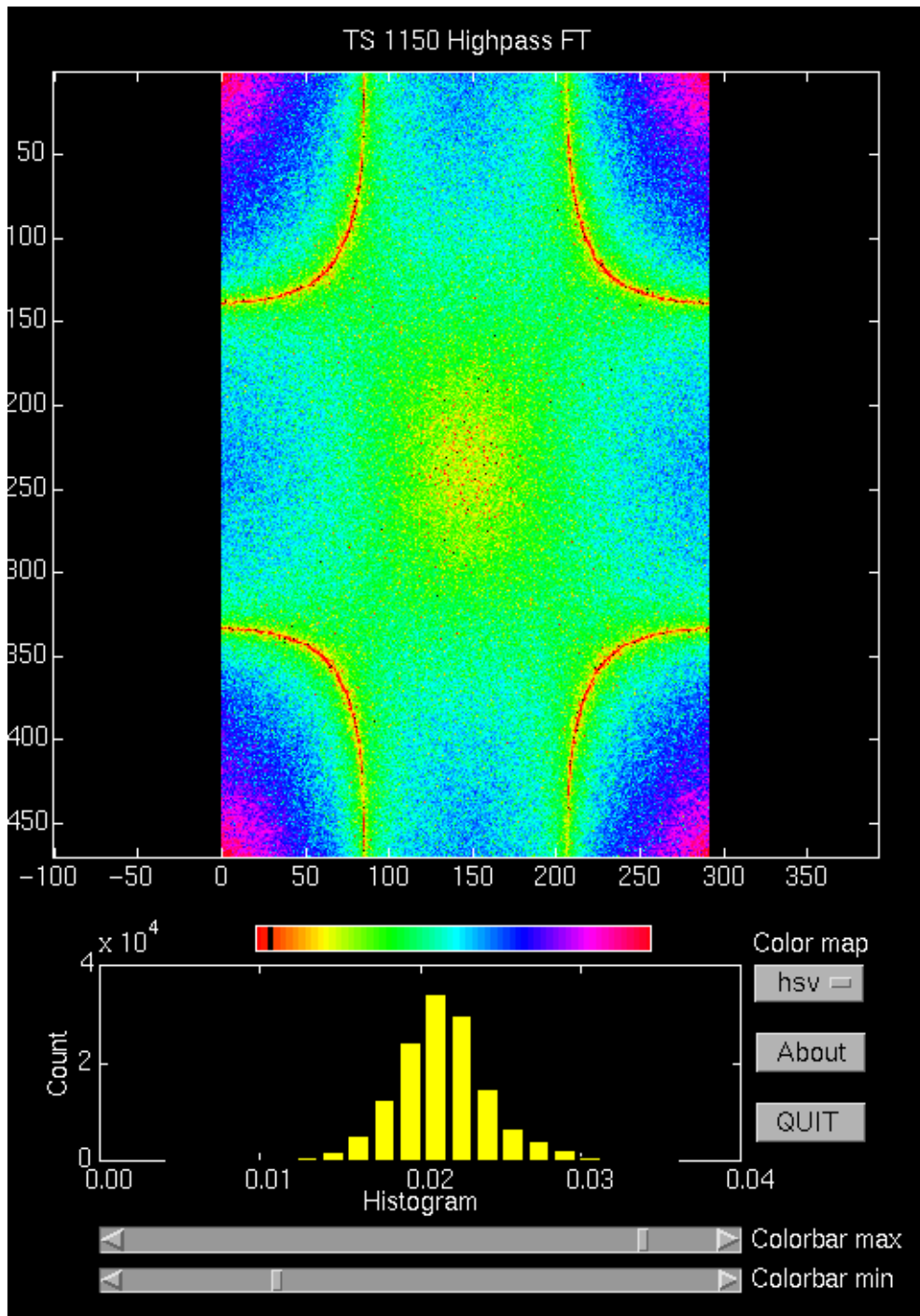


Figure 6. Sierra. Fourier spectrum Time Slice at 1150 ms filtered with highpass filter.

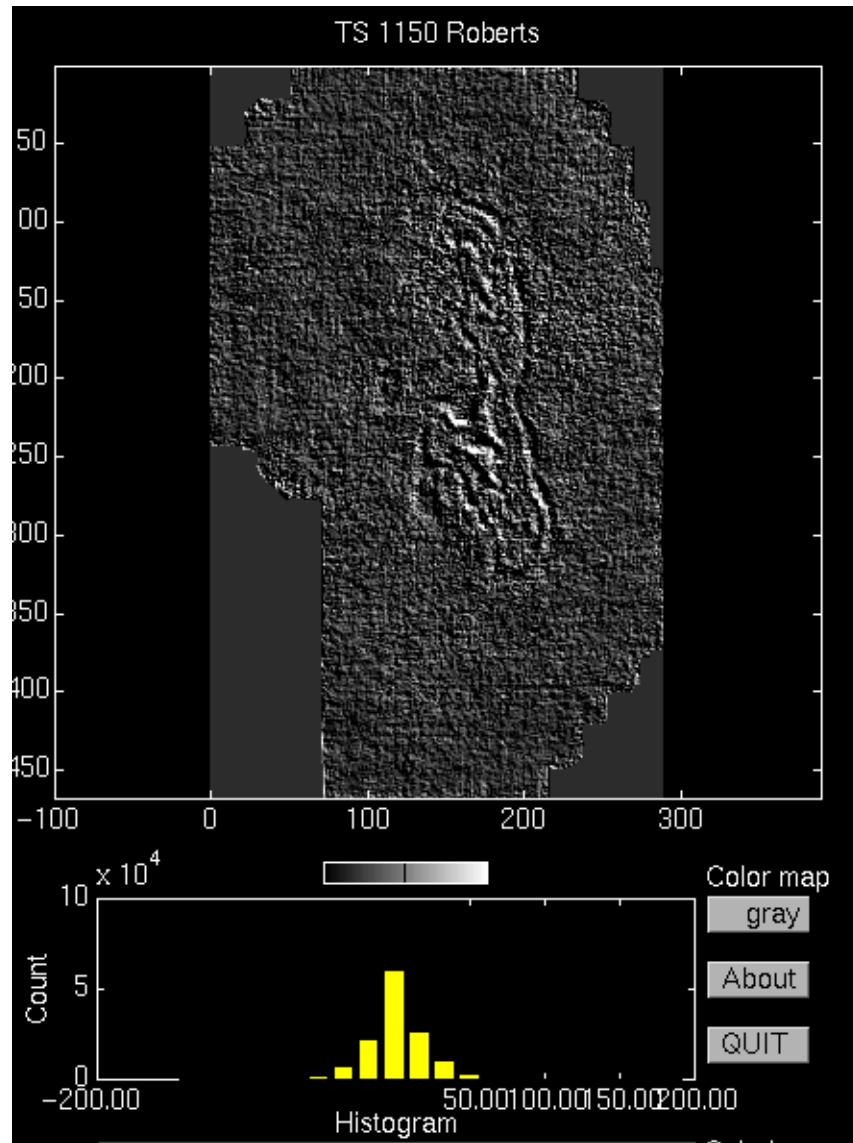


Figure 7. Sierra Time slice at 1150 ms: Roberts mask

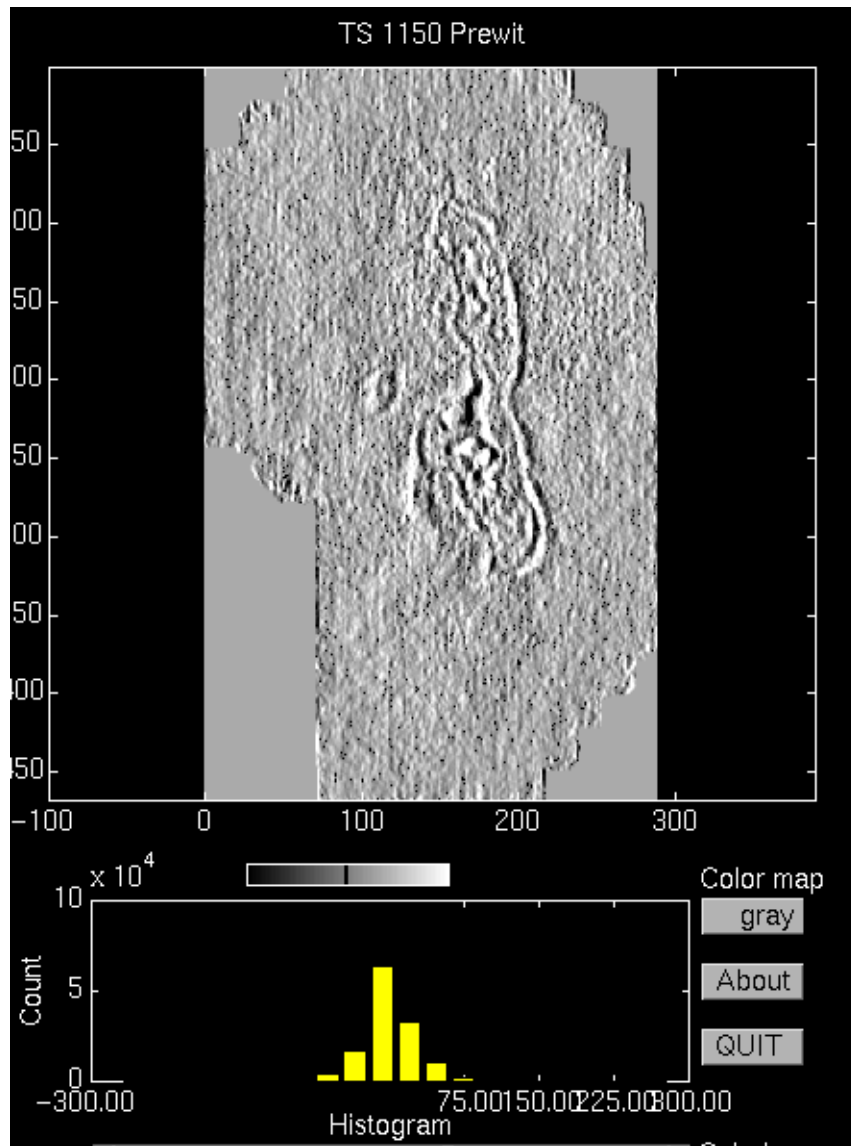


Figure 8. Sierra Time slice at 1150 ms: Prewitt mask

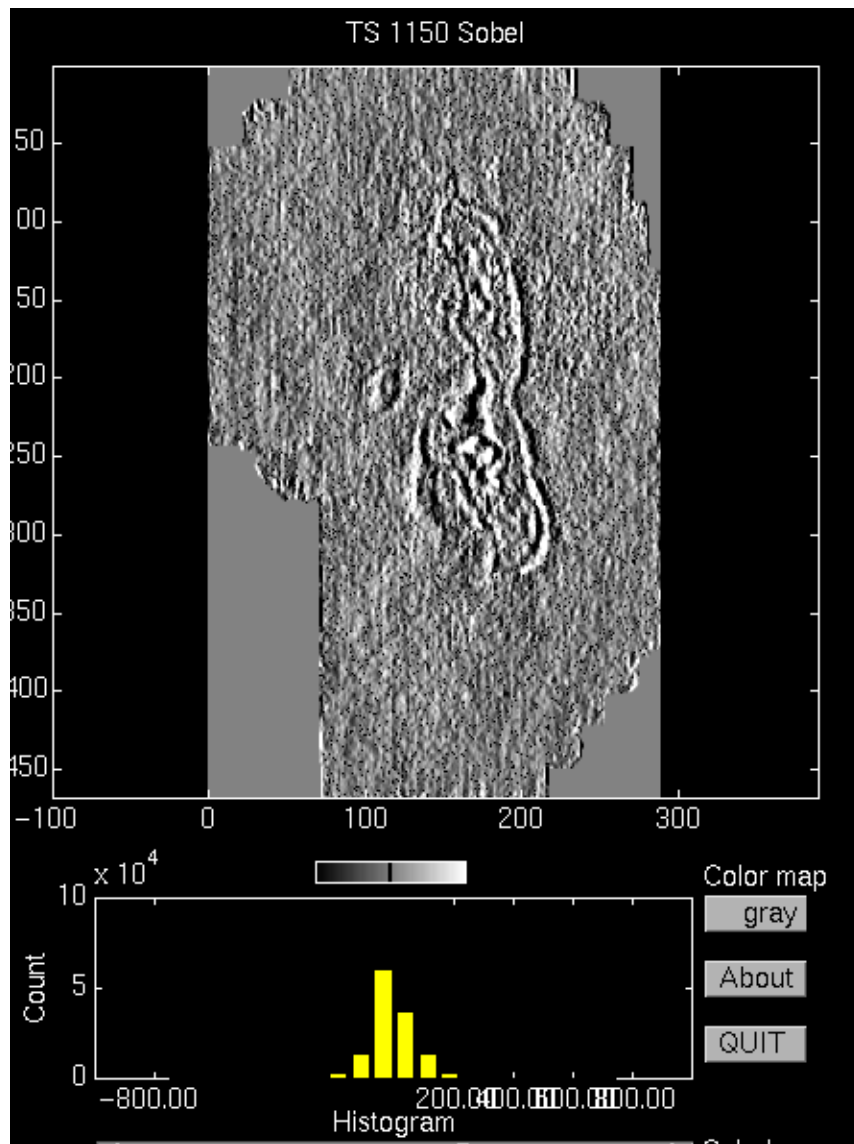


Figure 9. Sierra Time slice at 1150 ms: Sobel mask

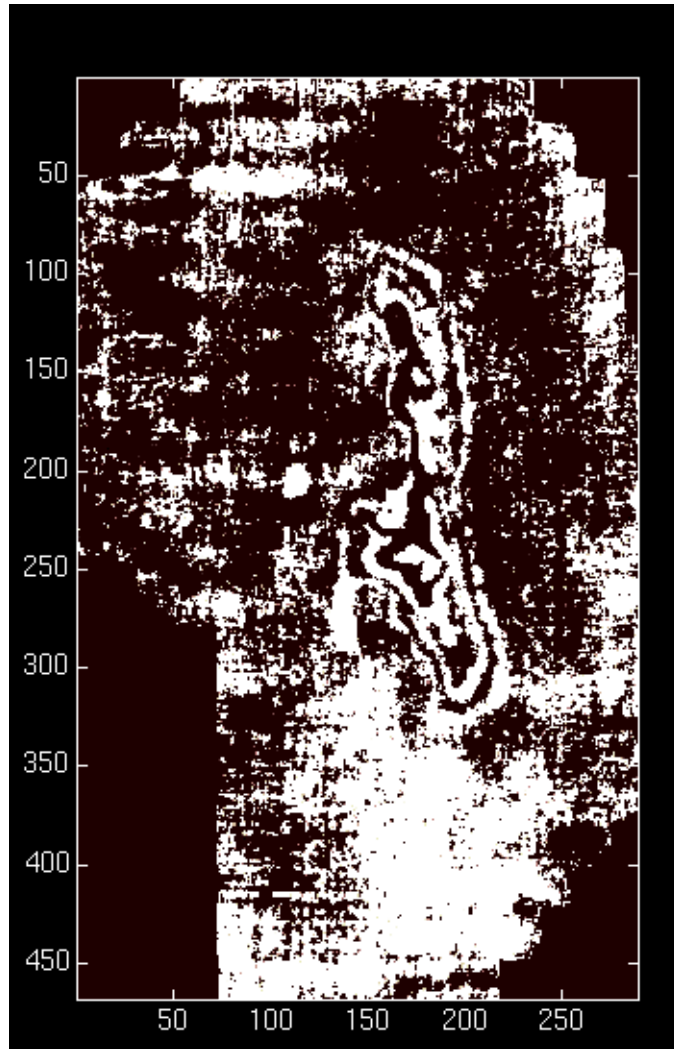


Figure 10. Sierra Averaged sum of five time slices 1100 - 1150 ms

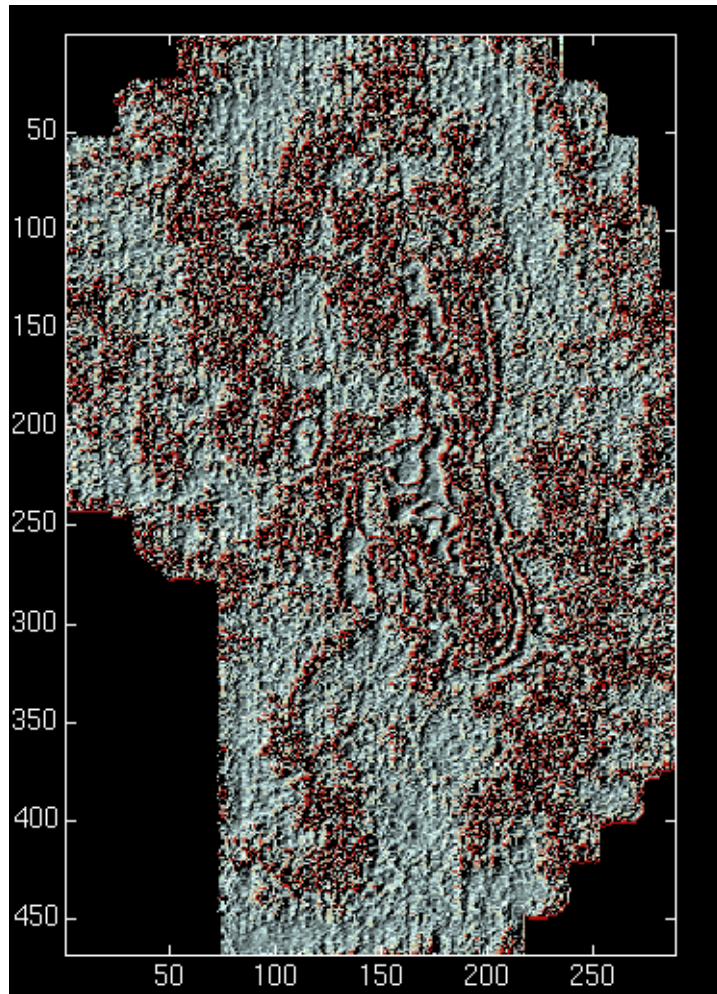


Figure 11. Sierra 1150 ms Coherency time slice